3rd Huixian International Forum on Earthquake Engineering for Young Researchers
August 11-12, 2017, University of Illinois, Urbana-Champaign, United States

Effect of Column Base Flexibility on the Hysteretic Response of Wide Flange Steel Columns

H. Inamasu[1], D.G. Lignos[2], A.M. Kanvinde[3]

1 *Doctoral Assistant, RESSLab, ENAC, Swiss Federal Institute of Technology, Lausanne (EPFL), Lausanne, Switzerland. E-mail: hiroyuki.inamasu@epfl.ch*
2 *Associate Professor, RESSLab, ENAC, Swiss Federal Institute of Technology, Lausanne (EPFL), Lausanne, Switzerland. E-mail: dimitrios.lignos@epfl.ch*
3 *Professor, University of California, Davis, Davis, United States of America. E-mail: kanvinde@ucdavis.edu*

ABSTRACT
Recent experiments on wide flange steel columns subjected to multi-axial cyclic loading underscore the influence of the member end boundary conditions on strength and stiffness deterioration due to coupling of local and lateral torsional buckling. Field observations complemented by recent tests indicate a similar sensitivity of response modes to the base flexibility. This paper investigates the effect of the column base flexibility on the hysteretic behavior of first story steel columns in moment resisting frames (MRFs). This is accomplished through rigorous finite element (FE) simulations, validated by full-scale column member and column base tests. Recent studies on embedded steel column base connections are used to infer the base flexibilities used in the FE simulations; these are representative of those commonly observed in first story interior columns of mid- to high-rise steel MRFs. The FE simulation findings indicate that column base flexibility delays the onset of local buckling, and subsequently reduces the axial shortening by about 50% compared to the fixed-base case. In contrast, the column base strength itself is insensitive to the column base flexibility.

KEYWORDS: *Column Base Flexibility, Embedded Column Bases, Wide Flange Steel Columns, Axial Shortening, Strength Deterioration*

1. INTRODUCTION

In recent years, a number of experimental and numerical studies investigated the hysteretic behavior of wide flange steel columns in moment resisting frames (MRFs) under multi-axial cyclic loading (Newell and Uang 2008; Elkady and Lignos 2015; Suzuki and Lignos 2015; Uang et al. 2015; Fogarty and El-Tawil 2016; Elkady and Lignos 2016; Elkady and Lignos 2017; Suzuki and Lignos 2017). These studies underscored the influence of a number of parameters on the column stability including (a) the local and global slenderness ratios; (b) the applied axial load; (c) the loading history sequence and (d) the member end boundary conditions. In all cases, the column was idealized to have a fixed base. This is a common assumption for columns embedded in a concrete footing (AISC 2012). Past experiments on embedded column base connections (Washio et al. 1978; Nakashima and Igarashi 1986; Grilli et al. 2017) suggest that the column base flexibility is not negligible in cases that the column is assumed to be fixed. This is due to the elastic deformation of the concrete subject to bearing stress, the steel base plate and the column embedded into the footing. Notably, reconnaissance reports from past earthquakes (Clifton et al. 2011; MacRae et al. 2015) as well as system-level numerical studies (Lignos et al. 2013) found that the partial fixity may be beneficial for the overall steel column seismic performance. Although the influence of the column base flexibility on the steel MRF response has been investigated through nonlinear response history analyses (Zareian and Kanvinde 2013), its influence on the column member hysteretic response has never been examined.

This paper investigates the effect of the embedded column base connection flexibility on the column hysteretic behavior through nonlinear finite element (FE) simulations. A continuum FE model representing the steel column is employed for this purpose. This model is validated with recent full-scale steel column tests (Elkady and Lignos 2017). The FE model is extended such that the column base flexibility is inferred on the basis of available full-scale tests on steel columns embedded in concrete footings (Grilli et al. 2017). The effect of the column base flexibility is highlighted by means of comparisons between the theoretically fixed model and the one that captures the column base flexibility.

Emphasis is placed on the effect of the column base flexibility on the column axial shortening due to the onset of local buckling near the column base.

2. FINITE ELEMENT MODEL DEVELOPMENT AND VALIDATION

A continuum FE model is developed to simulate the results from two steel columns that were recently tested at full scale (Elkady and Lignos 2016, 2017). Referring to Fig. 2.1, the column base was fixed but its top end was flexible. Table 2.1 summarizes the key geometric loading features of the employed test specimens. L_b/r_y (L_b and r_y are the unbraced length and the radius of gyration with respect to the weak-axis of the cross-section, respectively). Both specimens were subjected to a symmetric cyclic loading history about the strong axis coupled with a constant compressive axial load ratio, P/P_y (P is the applied axial load; $P_y = f_yA$; f_y is the expected yield stress; A is the column cross-section area). The FE model is developed in the commercial finite element analysis software ABAQUS (version 6.14-1) (ABAQUS 2014). A schematic view of the developed FE model is shown in Fig. 2.2. A more detailed discussion regarding the FE modeling approach is presented in Inamasu et al. (2017).

Figures 2.3 to 2.5 illustrate comparisons of the column base moment (M_{base}) – chord rotation (θ) relations; the axial (vertical) displacement at the column top (δ_v); and the deformed shapes obtained from the FE simulations and the test results. The second order moment demand has been subtracted in all cases. The chord rotation, θ, is defined as the horizontal displacement at the column top end divided by the actual column height, L after subtracting the corresponding column axial shortening, if any. All the definitions are shown in Fig. 2.1. The comparisons suggest that the developed FE model simulates relatively well the moment – chord rotation relation as well as the deformed shape and corresponding axial shortening throughout the entire loading history regardless of the employed cross-section.

Table 2.1 Selected column specimens for FE simulation and validation (Elkady and Lignos 2017)

Specimen ID	Cross -section	Slenderness ratio, L_b/r_y *1	Axial load ratio, P/P_y	Boundary conditions (Top-Bottom)	EI/L*2 (10^5 kNm/rad)
C3	W24x146	51	20%	Flexible - Fixed	0.923
C7	W24x84	79	20%	Flexible - Fixed	0.488

*1L_b/r_y: member slenderness (L_b unbraced length; r_y radius of gyration about weak-axis of the cross-section)
*2E: Young's modulus of steel material, and I: the second moment of inertia about the cross-section's strong axis

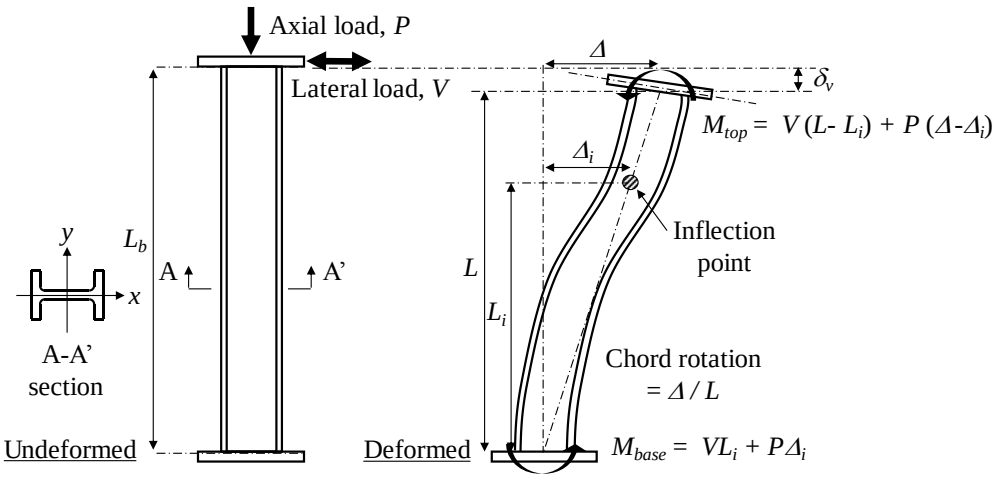

Figure 2.1 Schematic representation of member end boundary conditions

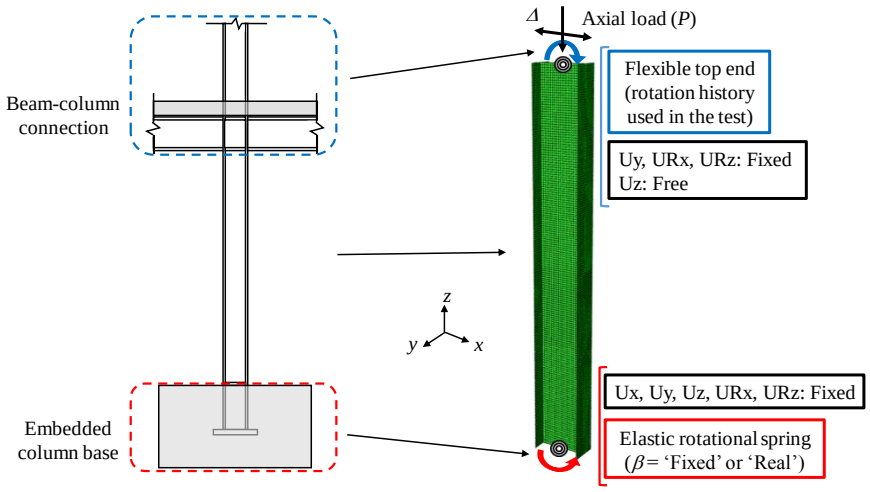

Figure 2.2 Finite element model representation of a first story embedded column base

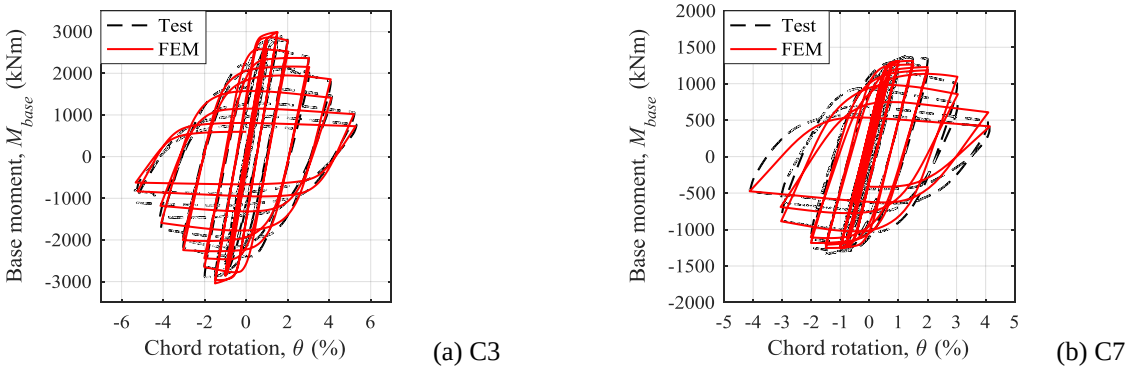

Figure 2.3 Base moment, M_{base} – chord rotation, θ relation obtained from tests and FE simulations (test data from Elkady and Lignos 2017)

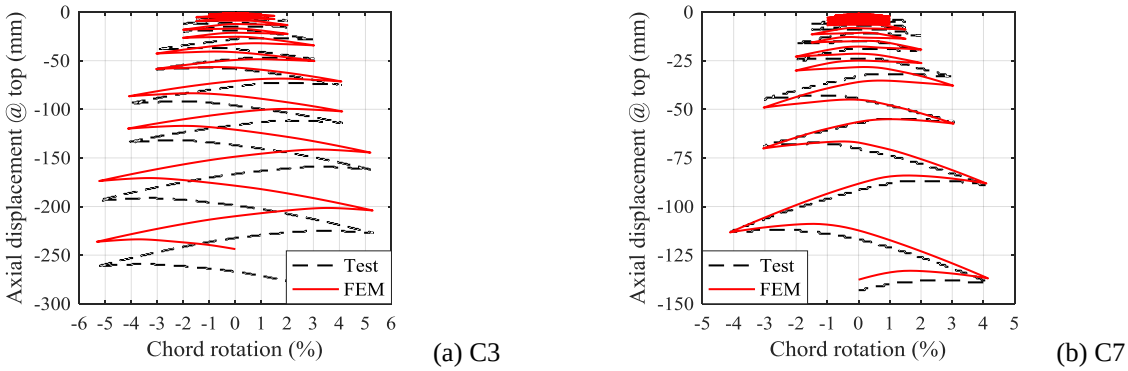

Figure 2.4 Axial displacement at the top – chord rotation, θ relation obtained from tests and FE simulations (test data from Elkady and Lignos 2017)

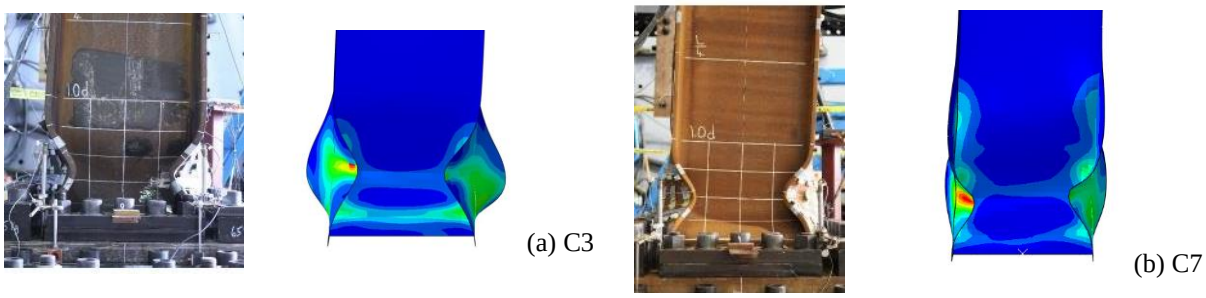

(a) C3 (b) C7

Figure 2.5 Deformed shape at 1st 4% chord rotation obtained from tests and FE simulations (images from Elkady and Lignos 2017)

3. COLUMN BASE FLEXIBILITY

Grilli et al. (2017) investigated the seismic performance of embedded column base connections subjected to compressive axial load and lateral drift demands. Columns were tested in a cantilever fashion. They were designed to remain elastic such that the observed failures were concentrated at the column base connection. Table 3.1 summarizes the main test parameters including the embedment depth, d_{embed}, and the applied compressive axial load. The same table summarizes the measured maximum flexural strength, M_{max} and rotational stiffness, β of the embedded column base connection after subtracting the elastic contribution of the respective column. Figure 3.1 illustrates the hysteretic response of a typical embedded column base connection. Figure 3.1 suggests that an embedded column base connection has an appreciable column base flexibility. The reported β values in Table 3.1 correspond to about 0.4 - 0.8% rotation under the design base moment. Notably, regardless of the column base flexibility, the specimens exhibited a considerable plastic deformation capacity without any strength loss.

Referring to Figure 3.1, the deduced β values of specimens #4 and #2 are used as the equivalent rotational stiffness of column specimens C3 and C7 in Table 2.1, respectively. These combinations are similar to those in practice considering that the column base connection is strong enough to transmit the column force demands. To simulate numerically the column base flexibility an elastic rotational spring is inserted at the column base of the FE model. The column base is assumed to have sufficient flexural strength to accommodate the column force demands without exhibiting inelastic behavior. It is noted that the embedded column base stiffness relative to the flexural stiffness of the column, $\beta / (EI/L)$ is 3.66 and 7.87 for C3 and C7, respectively.

Table 3.1 Summary of embedded column base connection test data (Grilli et al. 2017)

Specimen ID	Column cross-section	Column length (m)	P (kN)	d_{embed} (mm)	M_{max} (kNm)	β (10^5kNm/rad)
#1	W14x370	2.84	445	508	2613	3.23
#2	W18x311	2.84	445	508	2324	3.84
#3	W14x370	3.10	0	762	3741	3.07
#4	W14x370	3.10	445	762	4124	3.38
#5	W14x370	3.10	-667*	762	3800	3.25

* minus sign indicates tensile force

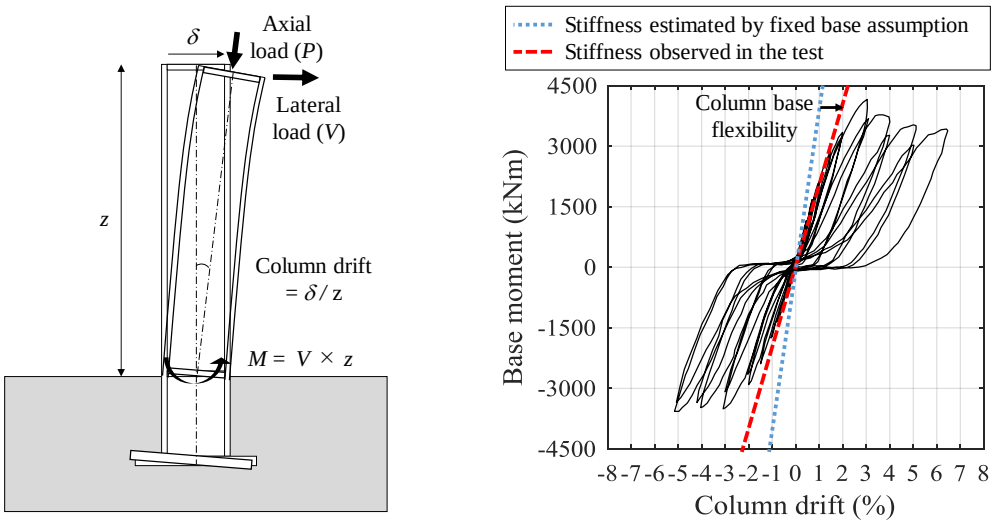

Figure 3.1 Deformed shape and representative hysteretic response of embedded column base connections (test data from Grilli et al. 2017)

4. EFFECT OF COLUMN BASE FLEXIBILITY ON COLUMN HYSTERETIC RESPONSE

Table 4.1 summarizes the examined cases through FE simulations. The β value only varies compared to the base cases. Referring to the same table, 'Fixed' is noted the theoretical fixed end column; while 'Real' refers to the β value estimated from the full-scale embedded column base tests. Therefore, the influence of the β value on the column cyclic behavior can be assessed by means of comparisons of 'C3-Fixed' with 'C3-Real', and 'C7-Fixed' with 'C7-Real'.

Shown in Fig. 4.1 is the base moment, M_{base}, – chord rotation, θ, relation for each one of the examined cases. Due to the embedded column base elastic contribution, in the "Real' cases the yield rotation angle and the rotation angle corresponding to the capping moment are larger than the equivalent "Fixed" cases. Notably, the attained capping moment is almost the same regardless of the column base flexibility. The column flexural strength degrades due to the formation of local buckling. The rate of cyclic degradation in flexural strength is practically not influenced by the column base flexibility; therefore, the column's flexural strength at a certain chord rotation after capping moment is slightly higher in the 'Real' case. This rate is strongly dependent on the cumulative plastic strain. Figure 4.2 shows the column top end moment, M_{top}, – chord rotation, θ, relations for the analyzed cases. From this figure, the column top end behavior is practically not influenced by the column base flexibility.

Table 4.1 All the examined cases in FE simulations

Model ID	Column cross-section	EI/L (10^5 kNm/rad)	β (10^5 kNm/rad)	β / (EI/L)
C3-Fixed	W24x146	0.923	∞	∞
C3-Real	W24x146	0.923	3.38	3.66
C7-Fixed	W24x84	0.488	∞	∞
C7-Real	W24x84	0.488	3.84	7.87

*minus sign indicates tension

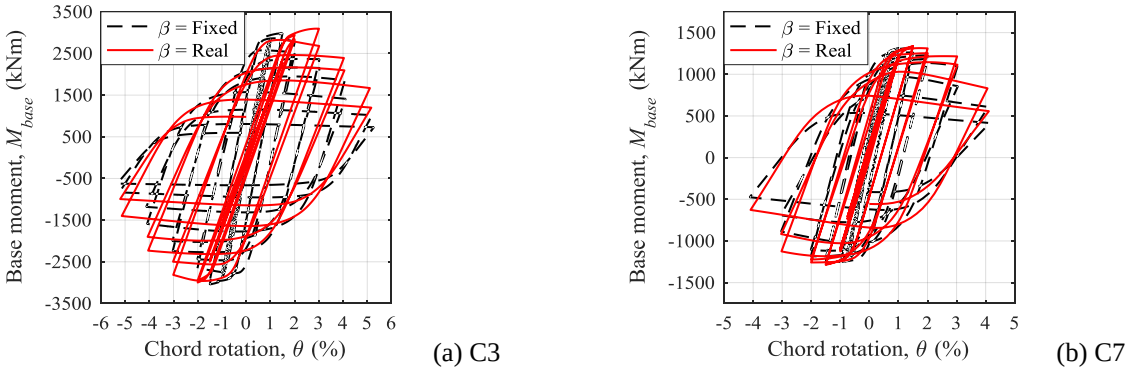

(a) C3 (b) C7

Figure 4.1 Effect of the column base flexibility in the base moment, M_{base} – chord rotation, θ relation

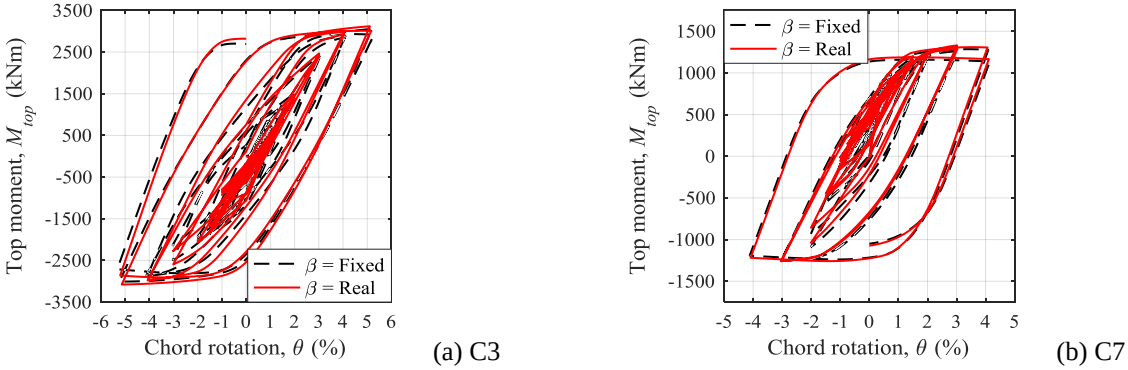

(a) C3 (b) C7

Figure 4.2 Effect of the column base flexibility in the top moment, M_{base} – chord rotation, θ relation

Fig. 4.3 shows the column axial shortening – chord rotation, θ, relation for the analyzed cases. The axial shortening is defined as the axial displacement at the column top. From this figure, it is evident that the column axial shortening at 4% drift is about 50% and 30% smaller than expected for C3 and C7 columns, respectively, when the column base flexibility is considered. Similarly, Fig. 4.4 shows the deformed shape at a drift ratio of 2% for the same cases with and without the column base flexibility. Elkady and Lignos (2015) found that the column axial shortening is associated with the cumulative plastic deformation of a column. The observed column axial shortening reduction in a 'Real' case is achieved because the cumulative plastic deformation at the certain rotation decreases due to the column base flexibility. This suggests that the current design assumption of a "fixed" column base may overestimate the column axial shortening.

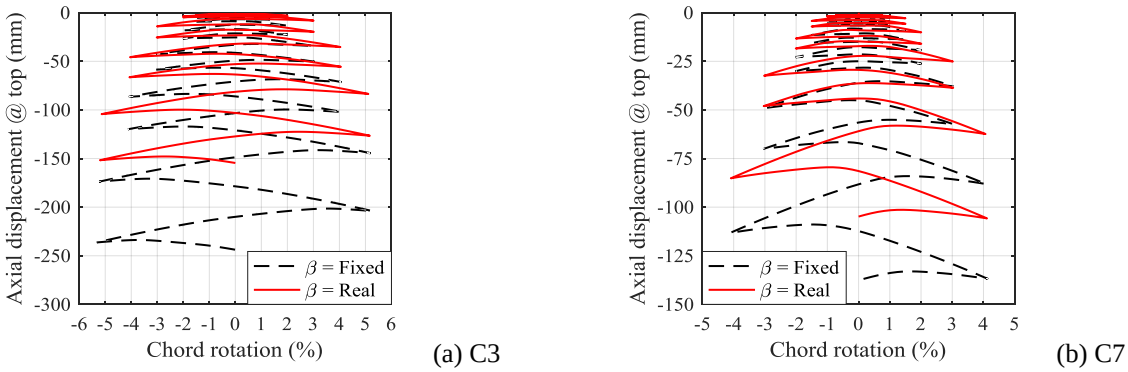

(a) C3 (b) C7

Figure 4.3 Effect of the column base flexibility in the top moment, M_{top} – chord rotation, θ relation

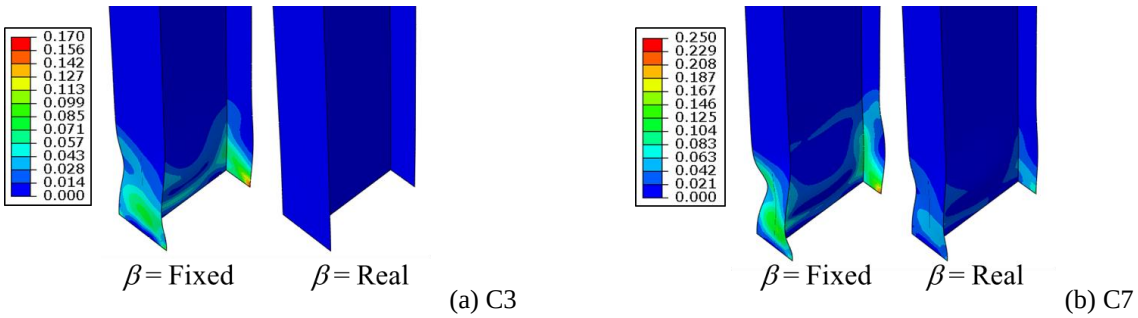

Figure 4.4 Effect of the column base flexibility in the local buckling deformed shape at 1st 2% chord rotation (contour indicates the cumulative plastic strain distribution)

5. CONCLUSIONS

This paper investigated the effect of the column base flexibility on the hysteretic behavior of first story interior wide flange steel columns in moment-resisting frames (MRFs). This was achieved through nonlinear finite element (FE) simulations that were validated based on data from full-scale column and embedded column base tests. Although the FE findings are still preliminary, the following observations can be made for the cases examined,

1. The yield rotation angle and the rotation angle corresponding to the capping moment of an embedded column base are larger than those expected in theoretically fixed column bases. This is mainly due to the reduction of the initial stiffness provided by the column base flexibility.
2. The attained capping moment as well as the rate of cyclic deterioration in column strength does not seem to be sensitive to the column base flexibility.
3. A fixed-base assumption seems to overestimate the column axial shortening by more than 50% at 4% lateral drift demands.
4. The column top end behavior does not seem to be influenced by the associated column base flexibility for the analyzed cases.

The authors are currently investigating the effect of column base flexibility on the column hysteretic behavior through a parametric study. A testing program has also been scheduled for this same purpose.

ACKNOWLEDGMENTS

This study is based on work supported by the Swiss National Science Foundation (Award No. 200021_169248). The financial support is gratefully acknowledged. Any opinions, findings, and conclusions or recommendations expressed in this paper are those of the authors and do not necessarily reflect the views of sponsors.

REFERENCES

1. ABAQUS. (2014). ABAQUS analysis user's manual version 6.14-1. Dassault Systems Simulia Corp., RI, USA.
2. AISC. (2012). Seismic Design Manual 2nd Edition. American Institute of Steel Construction.
3. Clifton, G. C., Bruneau, M., MacRae, G. A., Leon, R., and Fussell, A. (2011). Steel Structures Damage from the Christchurch Earthquake Series of 2010 and 2011. *Bulletin of the New Zealand Society for Earthquake Engineering*, **44:4**, 297–318.
4. Elkady, A., and Lignos, D. G. (2015). Analytical investigation of the cyclic behavior and plastic hinge formation in deep wide-flange steel beam-columns. *Bulletin of Earthquake Engineering*, **13:4**, 1097–1118.
5. Elkady, A., and Lignos, D. G. (2016). Dynamic Stability of Deep and Slender Wide-Flange Steel Columns - Full Scale Experiments. *The Annual Stability Conference*, Orlando, Florida, USA.
6. Elkady, A., and Lignos, D. G. (2017). Full-Scale Cyclic Testing of Deep Slender Wide-Flange Steel Beam-Columns under Unidirectional and Bidirectional Lateral Drift Demands. *16th World Conference on Earthquake Engineering (16WCEE)*, Santiago, Chile, num. 944.

7. Fogarty, J., and El-Tawil, S. (2016). Collapse Resistance of Steel Columns under Combined Axial and Lateral Loading. *Journal of Structural Engineering*, **142:1**, 4015091.
8. Grilli, D. A., Jones, R., and Kanvinde, A. M. (2017). Seismic Performance of Embedded Column Base Connections Subjected to Axial and Lateral Loads. *Journal of Structural Engineering*, **143:5**, 04017010.
9. Inamasu, H., Kanvinde, A. M., and Lignos, D. G. (2017). The Seismic Stability and Ductility of Steel Columns Interacting with Concrete Footings. *Composite Construction in Steel and Concrete VIII*, Jackson, Wyoming, USA.
10. Lignos, D. G., Hikino, T., Matsuoka, Y., and Nakashima, M. (2013). Collapse Assessment of Steel Moment Frames Based on E-Defense Full-Scale Shake Table Collapse Tests. *Journal of Structural Engineering*, **139:1**, 120–132.
11. MacRae, G. A., Clifton, G. C., Bruneau, M., Kanvinde, A. M., and Gardiner, S. (2015). Lessons from Steel Structures in Christchurch Earthquakes. *The 8th International Conference on Behavior of Steel Structures in Seismic Areas (STESSA)*, Shanghai, China.
12. Nakashima, S., and Igarashi, S. (1986). Behavior of Steel Square Tubular Column Bases for Interior Columns Embedded in Concrete Footings under Bending Moment and Shearing Force Part 1: Test program and Load-displacement relationships (In Japanese). *Journal of Structural and Construction Engineering (Transactions of AIJ)*, **366:1**, 106–118.
13. Newell, J. D., and Uang, C.-M. (2008). Cyclic Behavior of Steel Wide-Flange Columns Subjected to Large Drift. *Journal of Structural Engineering*, **134:8**, 1334–1342.
14. Suzuki, Y., and Lignos, D. G. (2015). Large Scale Collapse Experiments of Wide Flange Steel Beam-Columns. *The 8th International Conference on Behavior of Steel Structures in Seismic Areas (STESSA)*, Shanghai, China.
15. Suzuki, Y., and Lignos, D. G. (2017). Collapse Behavior of Steel Columns as Part of Steel Frame Buildings: Experiments and Numerical Models. *16th World Conference on Earthquake Engineering (16WCEE)*, Santiago, Chile, num. 1032.
16. Uang, C. M., Ozkula, G., and Harris, J. (2015). Observations from cyclic tests on deep, slender wide-flange structural. *The Annual Stability Conference*, Tennessee, Nashville, 247–263.
17. Washio, K., Suzuki, T., Nakashima, S., and Nishimura, I. (1978). Effect of Steel Column Embedment into Foundation at the Steel Column Base part 1: Experimental Results (In Japanese). *Summary of Technical Papers of Annual Meeting, AIJ, C-1(II)*, **53:1**, 1289–1290.
18. Zareian, F., and Kanvinde, A. (2013). Effect of Column-Base Flexibility on the Seismic Response and Safety of Steel Moment-Resisting Frames. *Earthquake Spectra*, **29:4**, 1537–1559.